INSTITUT D'AERONOMIE SPATIALE DE BELGIQUE

3 - Avenue Circulaire
B - 1180 BRUXELLES

AERONOMICA ACTA

A - N° 157 - 1976

Stratospheric balloon observations of the southern intertropical arc of airglow in the southern american area

by

G. WEILL and J. CHRISTOPHE
C. LIPPENS and M. ACKERMAN
Y. SAHAI

BELGISCH INSTITUUT VOOR RUIMTE-AERONOMIE

3 - Ringlaan
B - 1180 BRUSSEL

FOREWORD

Invited paper entitled "Stratospheric balloon observations of the Southern intertropical arc of airglow in the southern american area" presented at the 20e Symposium International d'Astrophysique in Liège. June 17-20. 1975.

AVANT-PROPOS

Cette communication intitulée "Stratospheric balloon observations of the southern intertropical arc of airglow in the southern american area" a été présentée sur invitation au 20e Symposium International d'Astrophysique à Liège du 17 au 20 juin 1975

VOORWOORD

Deze tekst genaamd "Stratospheric balloon observations of the southern intertropical arc of airglow in the southern american area" werd bij uitnodiging voorgedragen op het 20ste Internationaal Symposium voor Astrofysica gehouden te Luik van 17 tot 20 juni 1975

VORWORT

Der Vortrag "Stratospheric balloon observations of the southern intertropical arc of airglow in the southern american area" wurde zum 20ste Symposium International d'Astrophysique in Liège, 17.-20. Juni 1975 vorgestellt.

STRATOSPHERIC BALLOON OBSERVATIONS OF THE SOUTHERN INTERTROPICAL ARC OF AIRGLOW IN THE SOUTHERN AMERICAN AREA

by

G. WEILL and J. CHRISTOPHE*
C. LIPPENS and M. ACKERMAN**
Y. SAHAI***

* *Institut d'Astrophysique de Paris*
** *Institut d'Aéronomie Spatiale de Belgique*
*** *Instituto de Pesquisas Espaciais*

Abstract

Multicolor spectral observations of the intertropical arc over a large area are reported from a stratospheric balloon flying over Brazil. The structure of thermospheric 5577 emission is clearly distinguishable from the lower altitude emission layer. 5577/6300 intensity ratios can be used as a sensitive height indicator for the dissociative recombination layer. A determination is made of the branching ratio of ionospheric recombination into the ^1S and ^1D metastable states of OI. The peak ionization in the anomaly is positioned in space through the emission of 7774 permitted OI lines. The spatial separation of the allowed and forbidden emission regions is variable and sometimes exceeds 300 km. It implies that the spread of ionization in the anomaly is also variable and sometimes considerable.

Résumé

Des observations dans plusieurs couleurs des arcs intertropicaux au-dessus d'une vaste étendue géographique ont été effectuées par ballon au-dessus du Brésil. La structure de l'émission thermosphérique à 557.7 nm peut être clairement distinguée des émissions à plus basse altitude. Les rapports d'intensité 5577/6300 peuvent être utilisés comme indicateur de l'altitude de la couche de recombinaison dissociative. Les taux de recombinaison dans les niveaux ^1S et ^1D de l'oxygène atomique sont déterminés. Le maximum d'ionisation dans l'anomalie est localisé dans l'espace au moyen de l'émission des raies permises de OI à 777 4 nm. La séparation spatiale des régions d'émission permise et interdite varie et dépasse parfois 300 km. Il apparaît que l'ionisation dans l'anomalie s'étend de façon variable et est parfois considérable.

Samenvatting

Waarnemingen in verschillende kleuren van intertropicale bogen boven een uitgestrekt geografisch gebied werden per ballon verricht boven Brazilië. De structuur van de thermosferische uitstraling bij 557.7 nm kan duidelijk onderscheiden worden van de emissies voorkomende van geringere hoogte. De verhoudingen van de intensiteit 5577/6300 kunnen gebruikt worden als hoogte aanduiding voor de laag van dissociatieve recombinatie De waarde van de recombinatie in de niveau's ^{1}S en ^{1}D van atomaire zuurstof werden bepaald Het maximum van ionisatie in de anomalie werd vastgelegd in de ruimte door middel van de emissie van de toegelaten lijn van OI bij 777.4 nm. De scheiding in de ruimte tussen de gebieden met toegelaten en met verboden emissie verandert en bedraagt soms meer dan 300 km. Schijnaar spreidt de ionisatie in de anomalie. die soms belangrijk kan zijn. zich uit op een veranderlijke manier.

Zusammenfassung

Vielfarbige Spektralbeobachtungen des Intertropicalbogens wurden über ein grosses Feld von einem stratosphärischen Ballon über Brasilien gemacht. Die Struktur des 557.7 nm thermosphärischen Himmelsleuchtens kann von dem Himmelsleuchten der unteren Schichte unterschieden werden. Das Intensitätsverhaltnis 557.7/630.0 kann als Höhezeichen der dissoziativen Rekombinationsschichte gebraucht werden. Das Verhältnis der Rekombination in die ^{1}S und ^{1}D Zustände von OI wird festgestellt Die Maximumionisation in der Anomalie wird im Raum durch die 777.4 nm Emission von OI festgestellt. Die Raumtrennung zwischen erlaubten und verbotenen Linien ist veränderlich und manchmal grösser als 300 km. Die Verteilung der Ionisation in der Anomalie ist deswegen auch veränderlich und manchmal sehr gross.

Intertropical arcs of night airglow (1) have now been studied for fifteen years, from space (2) and earth. Satellite observations have provided a global picture of the emission (OGO) and of related electron densities (Alouette, ISIS). Forbidden transitions of OI are due to dissociative recombination; the distribution of which is governed by the effects of ambipolar diffusion and neutral winds in the low - dip magnetic field. After the unexplained observation of an OI permitted line at 4368 Å (3), the resonant line at 1304 Å and the 1356 Å line were observed by satellite and associated with the Appleton anomaly of ionization (4). The 7774 radiation was later observed from the ground in the intertropical zone (5), (6). The main process responsible for exciting higher energy OI levels appears to be radiative recombination

(a) $O^+ + e^- \rightarrow O^*$

with possibly a small contribution from ion-ion recombination

(b) $O^+ + O^- \rightarrow 2\,O^*$

Despite this progress in understanding, the space distribution of the various emissions had not yet been clearly established, we undertook some observations from stratospheric balloons, expecting that this vehicle would present, with respect to orbital or ground observatories, the following advantages :

a) practical elimination of atmospheric absorption and scattering effects, in the optical window of interest.

b) latitude coverage larger than the scale of the structure, through the use of horizontal sightings.

c) improved ratio of atmospheric signal to extra terrestrial light.

d) separation of variations with space and time.

The photometric gondola (10) was constructed in collaboration between Institut d'Aéronomie Spatiale de Belgique and Institut d'Astrophysique de Paris. It is a classical filter turret photometer which takes horizontal sightings with a 3^0 hight by 6^0 azimuth

field. The whole instrument is rotated around a vertical axis at about 6^0/sec. Ten interference filters, dark current and internal calibration are placed sequentially, every minute on the optical axis. The turret is under thermostatic control while the trialcaline photomultiplier is cooled by the ambiant environment. The photometric signal is recorded on the ground by FM/PM telemetry with three different amplification levels, together with a number of thermal and electrical control data. The attitude is measured by X and Y magnetometers. The attitude can be verified by star crossings. Such crossings provide a check that any pendular movements under the balloon are well within the vertical angular resolution.

In order to retain the full spatial resolution of the instrument, the signal is integrated over each 3^0 azimuth interval.

We took advantage of an astronomical balloon launching campaign organized by Centre National d'Etudes Spatiales to fly a balloon in the southern tropical region, in the vicinity of the Brazilian magnetic anomaly. In connection with particle precipitation on the eastern side of the anomaly (11), strong emission effects had been expected in this area, so far not conclusively confirmed by airborne (12) and satellite borne photometry, in satellite particle precipitation has impaired the use of photomultipliers in the area.

The balloon was floating at 38 kilometers ceiling altitude on February 27th 1973 from 0h 30 mn to 3h 55 mn U.T., drifting at 110 km/hr towards the East North East. The distance to the magnetic equator was - 13.1^0 and- 10.4^0 at the beginning and end of the ceiling, respectively (Fig. 1). The flight was entirely nocturnal, as the solar height was - 37.4^0 at ceiling start. A typical reduced scan is shown on figure 2.

For brevity, the 7774, 6300 and 5577 emission features will now be referred to by "IR", "R", and "G", respectively. "DR" and "RR" will stand for "Dissociative Recombination" and "Radiative Recombination" respectively.

The R arc is clearly observed during the whole flight in fairly stable directions $75^0.3 \pm 7^0$ (West) and $247^0 \pm 7^0$ (East). Its semi-width at half intensity is about 12^0 of

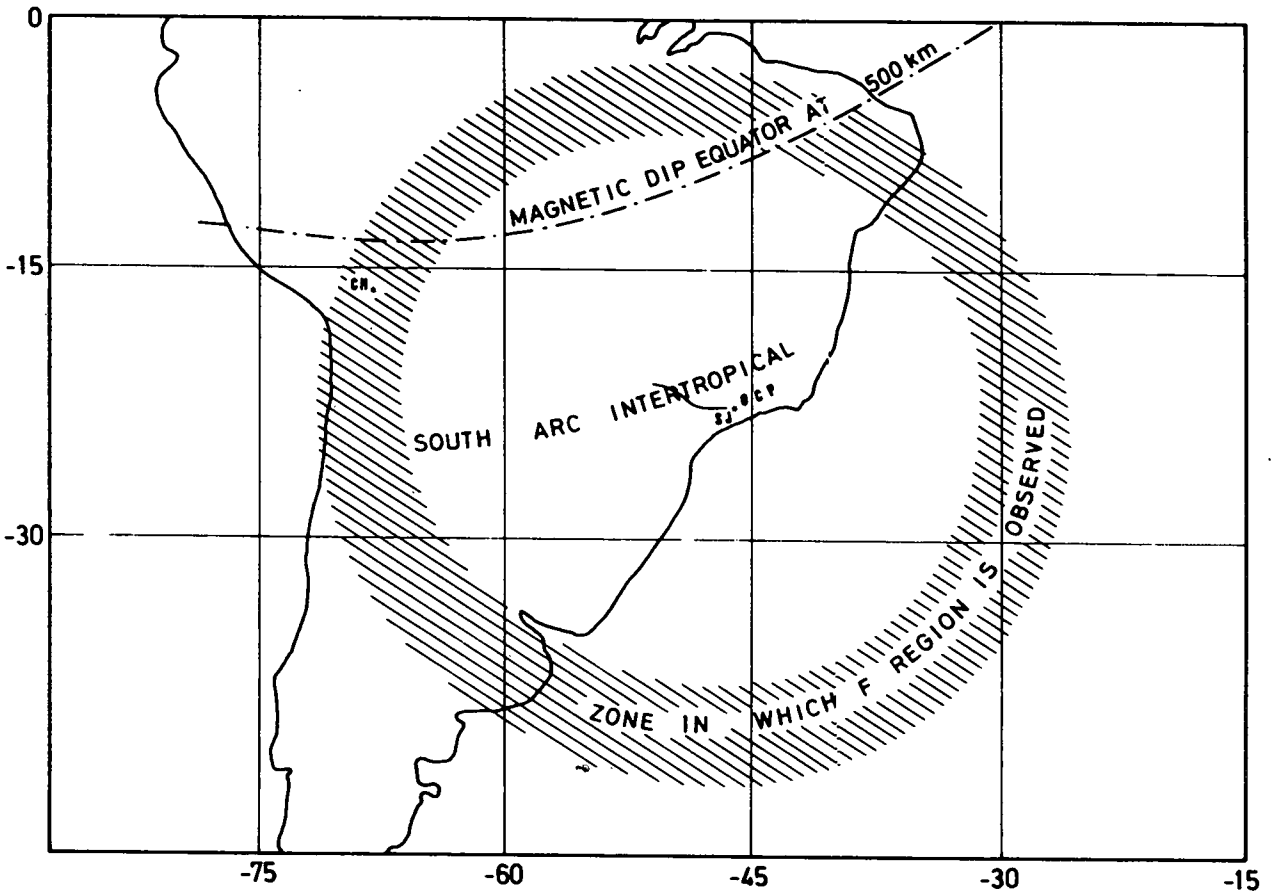

Fig. 1.- *General area of observation.*

The area shown X is fixed by the extreme heights of thermospheric observations involved (250 to 420 km) and by the comparatively small balloon drift. The magnetic apex equator for 500 km (13) is shown. The launch site Sao José dos Campos (SJ) and ionospheric station Cachoeira Paulista (CP) are shown, and also Chacaltaya (CH) in tribute to a precursor.

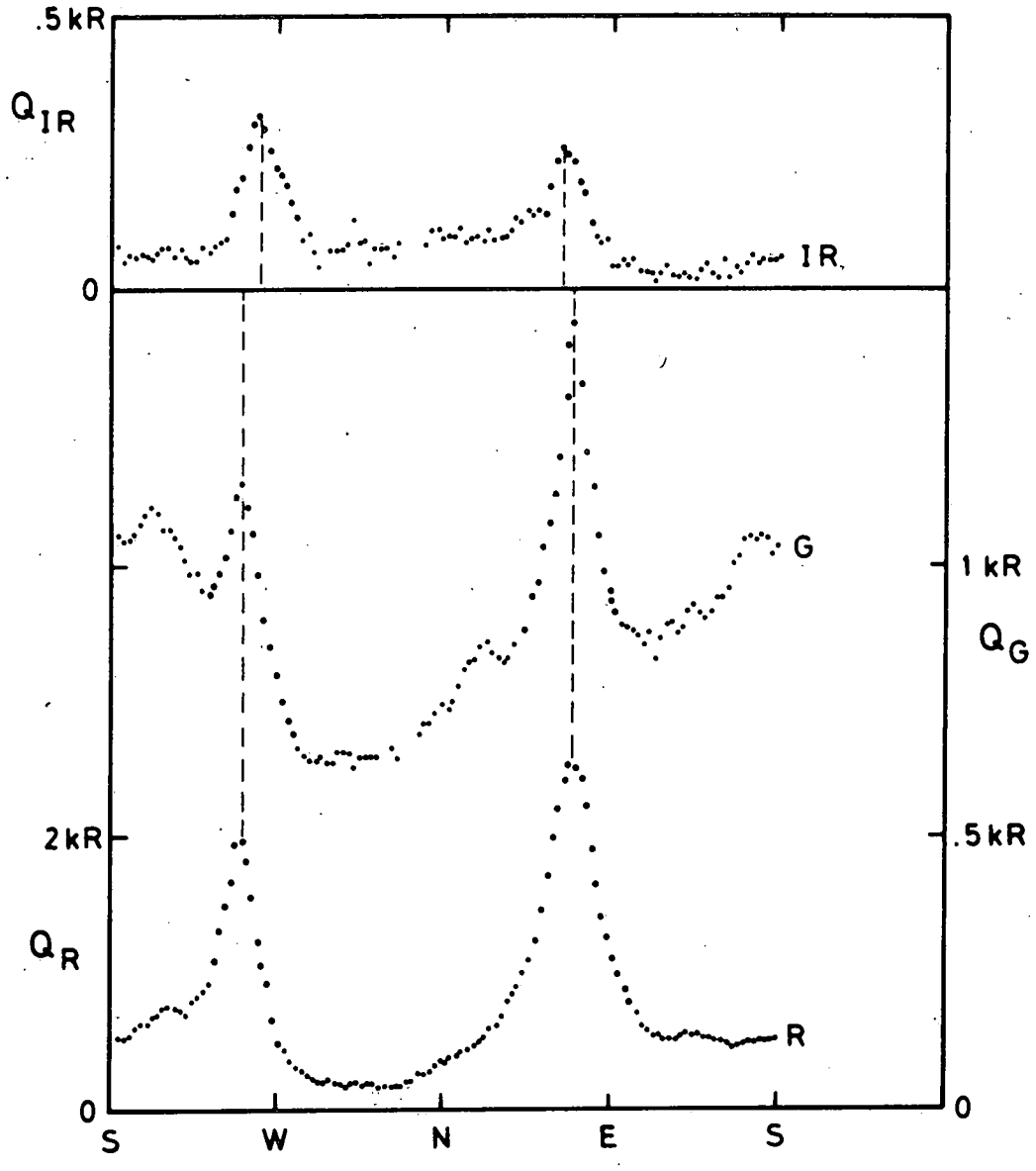

Fig. 2.- *A typical horizon scan showing 3 oxygen radiations :*

R	6300 Å	(^{3}P - ^{1}D)	1h 46 mn 40 sec	1h 47 mn 48 sec
G	5577 Å	(^{1}D - ^{1}S)	1h 50 mn 00 sec	1h 51 mn 07 sec
IR	7772 + 7774 + 7775	(3^5S^0 - 3^5P)	1h 43 mn 20 sec	1h 44 mn 27 sec

The curve is not decontaminated for the lower altitude emission. Units are absolute slant intensities (10^6 quanta/cm^2 x sec or Rayleighs).

azimuth on the poleward side of the maximum (Fig. 3a). On the equatorward side. it is much wider on the eastern than on the western section. Moreover, figure 3b indicates that the latitudinal spread varied with local time, decreasing in the early night hours and increasing sharply about local midnight.

The G arc is also clearly observed despite the interference of the lower 5577 emission layer which follows its own and presumably unrelated latitude variation. The G and R coincide in azimuth within the accuracy of determination. The average displacement is R to the North of G by $.2 \pm .4^0$.

In contrast, the IR peaks are significantly displaced by 2 to 12^0 azimuth always to the North of the R peaks; higher displacements are observed on the western than on the eastern section; for both sections the angular separation is at a maximum about 02h U.T.

This morphology can be qualitatively understood with the help of a model (Fig. 4). It is controlled by the electron distribution in the area, itself controlled by the magnetic and gravity fields. The IR arc of radiative recombination peaks at the N_{emax} whereas the G arc due to dissociative recombination peaks at $([O_2][e^-])_{max}$, directly below on the same magnetic shell. The height dependant effect of quenching on the R arc is to raise it above the G peak; model calculations show that this displacement will typically be only a few kilometers, which is consistent with the observations.

Absolute intensity ratios between two radiations for each arc intercept are established by least square analysis of intensities observed in a 60^0 sector around each individual peak. Determinations are retained only if the correlation coefficient between the two profiles is high. This coefficient c is better than .95 for 60% of all determinations, and falls below .8 only toward the end of the observing period when the arc is considerably weakened in the East. The R intensities are known to be due almost entirely to dissociative recombination (14)

$$(c) \qquad O_2 + e^- \rightarrow O^+ + O^*$$

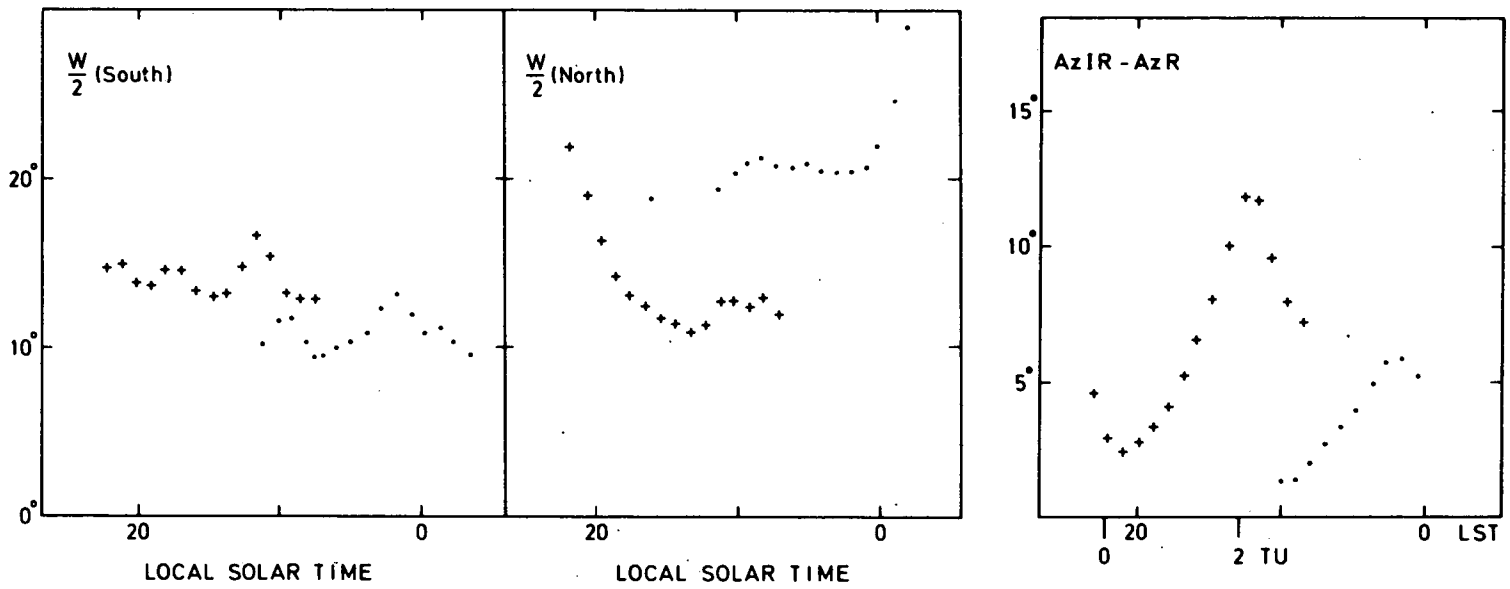

Fig. 3.- *Angular widths and separation of the arcs.*

a) semi angular widths at half intensity of the R arc (poleward side)

b) the same for the equatorward side

c) azimuth separation of the IR and R arcs. The IR arc is always displaced to the North

+ for western section

∘ for eastern section

The raw data have been smoothed by a three-point running mean.

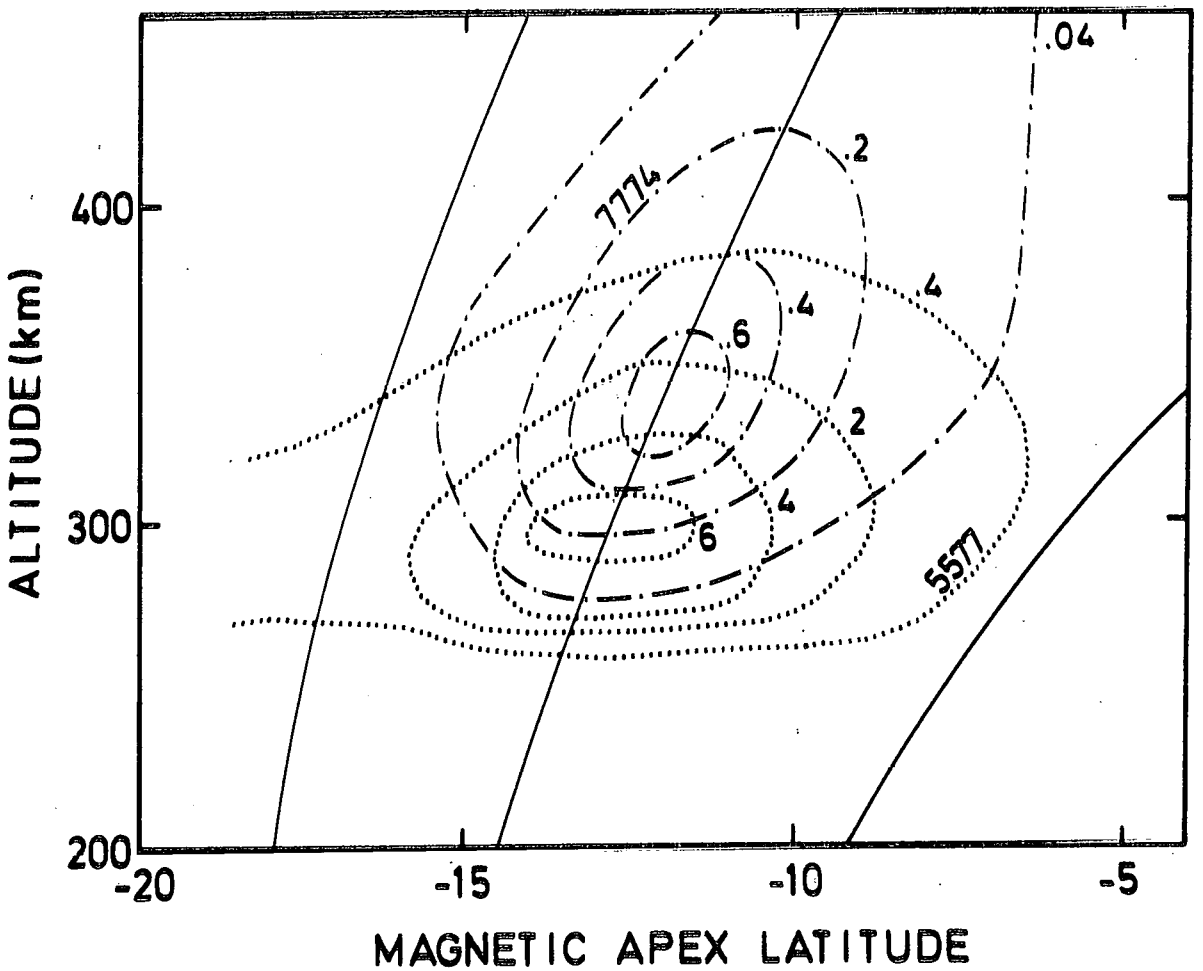

Fig. 4.- *Sketch of Meridional cross section of G and IR volume emissivities in the anomaly.*
A distorted presentation height versus latitude (compressed). Neutral atmospheric Model. "US Standard Atmosphere Supplements" Spring Fall, 900°K.
Electron distribution : vertical Chapman distribution, H = 30 km peak density 10^6 electron/cc with empirical weighting as a function of magnetic apex altitude. Isophotes in quanta/cc x sec.

with possibly minute contributions from

(d) $NO^+ + e^- \rightarrow N + O^*$

and from Ion - Ion recombination (b) which need not be taken into account. R is therefore taken as a reference in order to establish the G and IR arc intensities through the above mentioned regression analysis followed by a parabolic interpolation to the time of the R scans. The procedure largely eliminates the uncertainties due to the G lower emission layer (100 km) and to the strong spectral background around the IR lines. When comparing IR to R the best fit is obtained by regressing IR/R^a with $a = 2.0 \pm .5$. This is consistent with an RR source for IR (volume emissivities proportional to $[e^-]^2$, whereas they are proportional to $[e^-]$ for DR. The time variation of peak intensities in the Western and Eastern sectors is shown on Fig. 5.

The observed G/R intensity ratio is far from constant with time. it varies between .18 and .39. With dissociative recombination, this ratio of integral intensities is insensitive to the height profile and, to an excellent approximation, equal to the ratio of volume emissivities at the emission peak altitude, which writes

$$\text{(e)} \qquad \frac{G}{R} \cong \left(1 + \frac{S_{N_2}[N_2]}{A(^1D)} + \ldots\right) K(^1S) \frac{A_G}{A(^1S)} \Bigg/ K(^1D) \frac{A_R}{A(^1D)}$$

where (see, for instance, (14), or (15), for further references and numerical values)

S_{N_2} is the quenching coefficient of $O(^1D)$ by N_2.

$K(^1S)$ is the number of 0 atoms in the (^1S) state produced by each $O^+ + O_2$ reaction.

$K(^1D)$ is the number of 0 atoms in the (^1D) state produced by each $O^+ + O_2$ reaction (including cascading from the (^1S) line.

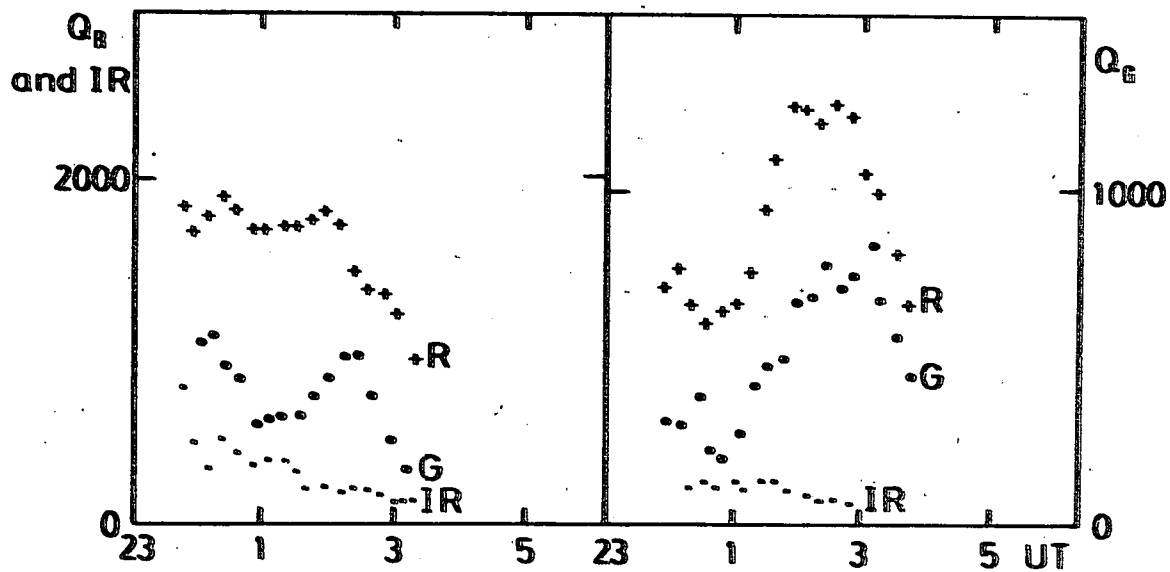

Fig. 5.- Peak intensities (Rayleighs) of the IR, G and R intensities in the eastern and western sections of the arc, as a function of time.

A_G, A_R are the transition probabilities for the 5577 and 6300 lines. respectively.

$A(^1S)$, $A(^1D)$ are the Einstein coefficients for the (^1S) and (^1D) states. respectively.

In the parenthesized quenching term in (e). using currently accepted values of the parameters. the electron quenching term may be omitted. as it is. under the ionospheric conditions concerned, negligibly small before Nitrogen quenching.

G/R should therefore provide a sensitive measurement of N_2 concentration at the peak dissociative recombination level, or, given a model of the neutral atmosphere of the peak emission altitude. A comparison of G/R and the virtual height of the F layer h'_F at Cachoeira Paulista ($22^0.7$ S, $45^0.2$ W) as a function of time does show a correlation as good as can be expected in view of the large longitudinal distance between the optical and ionosonde observations, and of the systematic separation between the peak dissociative recombination altitude and h'_F. This correlation can, however, be used to extrapolate G/R to null N_2 concentration (Fig. 6): *in the absence of quenching, dissociative recombination of O^+ in the ionosphere would produce 5 ± 1 quanta at 6300 A for each 5577 A quantum*. A comparison of G/R to computed profiles of the bottom-side $[e^-]$ distribution is underway: it may provide a good determination of the quenching factor S_{N_2} : in the present work we shall adopt 2.10^{-11} as a temporary value.

We can now derive the altitude of maximum dissociative recombination rate of R region ionization from G/R observed ratios by means of equation (e). We interpolate the US Standard Atmosphere Supplements (1966) tables (Spring/Fall model), for N_2 concentrations, and neglect other quenching agents than N_2.

From the geographical position of the R maximum intersect, we trace the magnetic field line onto the apex altitude Z. We than assume that the R and IR arcs are locally on the same apex shell (13) and derive the altitude h_{IR} and magnetic apex latitude φ_{IR} from the direction in which the IR peak is observed. The line of maximum IR emission can thus be

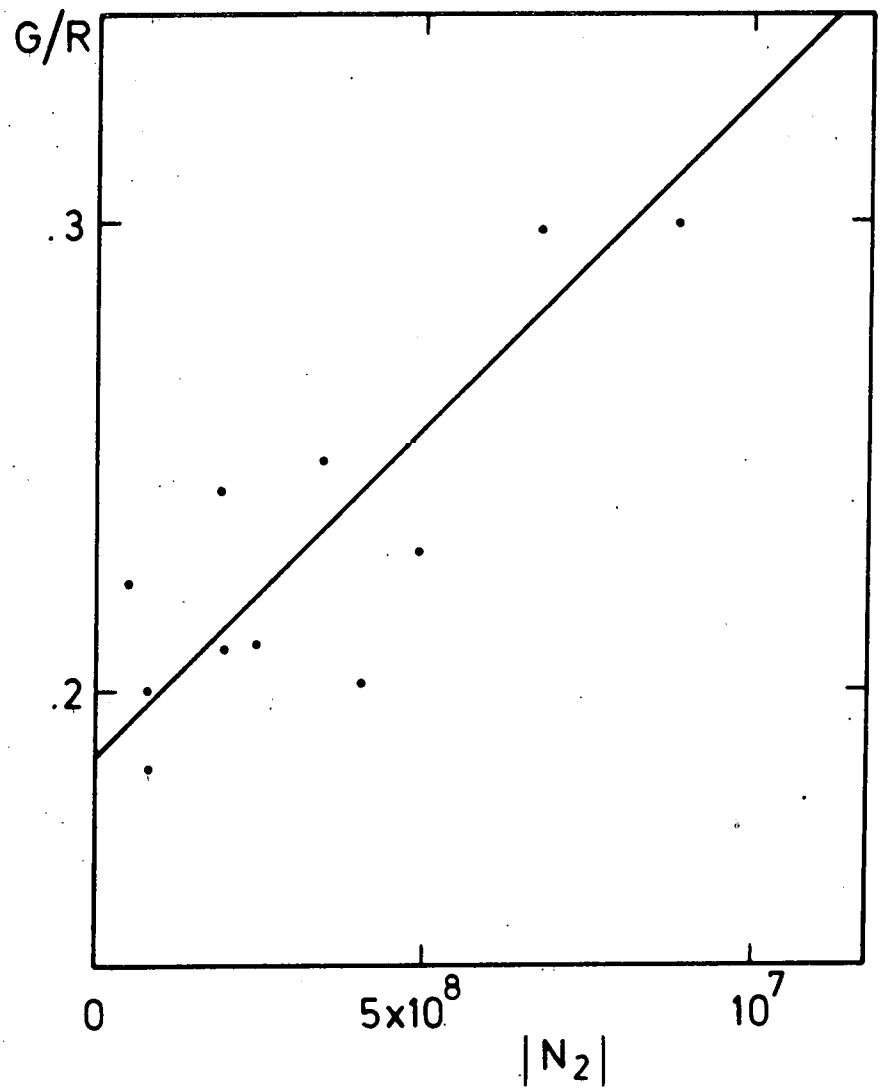

Fig. 6.- *Thermospheric G/R integral intensity ratio, East-West average versus N_2 densities (molecules/cc) at h'_F, at Cachoeira Paulista.*
(from "US Standard Atmosphere Supplements", Spring Fall Model, interpolated for relevant exospheric temperature, same Model.). Generally $h'_F < H_G$; the regression slope should therefore not be taken as a measurement of S_{N_2} (see text).

completely positioned both in altitude and latitude. The results of this procedure are shown on Fig. 7 for the western and eastern sections. The line of IR_{max} probably did not pass over Cachoeira Paulista during the optical observation period, but remained 100 to 200 kilometers to the North of it. The variation of $f_o F_2$ seems to reflect the variable distance to the ionization peak rather than the peak electron content. The maximum electron concentration observed by the ionosonde was 1.5×10^6 el. cm^{-3} at 1.30 U.T., when the IR peak line was closest (about 100 kilometers). Magnetic declination is high in the 30° West longitude sector, whereas it is low in the 65° West sector; the effect of thermospheric winds on the ionization structure may therefore be quite different and account for the different behaviours of the Eastern and Western sections of the arc.

A striking fact in the data is the high and variable separation between the IR and R arcs. The maximum distance between the maximum intensity lines is about 320 kilometers along a field line, and the altitude separation varies from 10 to 90 kilometers in the East, 25 to 140 kilometers in the West. Such separations cannot be reconciled with an empirical Chapman ionospheric layer.

$$\frac{Ne}{Ne\ max} = \exp \frac{1}{2} \left[1 - \frac{h - h_m}{H_e} - \exp - \frac{h - h_m}{H_e} \right]$$

where the scale factor H_e is the scale height of atomic oxygen. Several authors (15) and (16) have recently proposed that simultaneous observations of oxygen permitted and forbidden transitions in the tropical night airglow be used to derive F region height and N max. The use of a Chapman type electron districution with H_e = H(O) is a very coarse in the anomaly region where, in view of the large spatial separation between the regions involved by the emission of forbidden and permitted lines, the method is apt to produce unreliable results.

In a forthcoming paper, we shall further exploit the data presented here in order to map the structure of ionization in the anomaly and to derive the rates of the ionospheric reactions concerned.

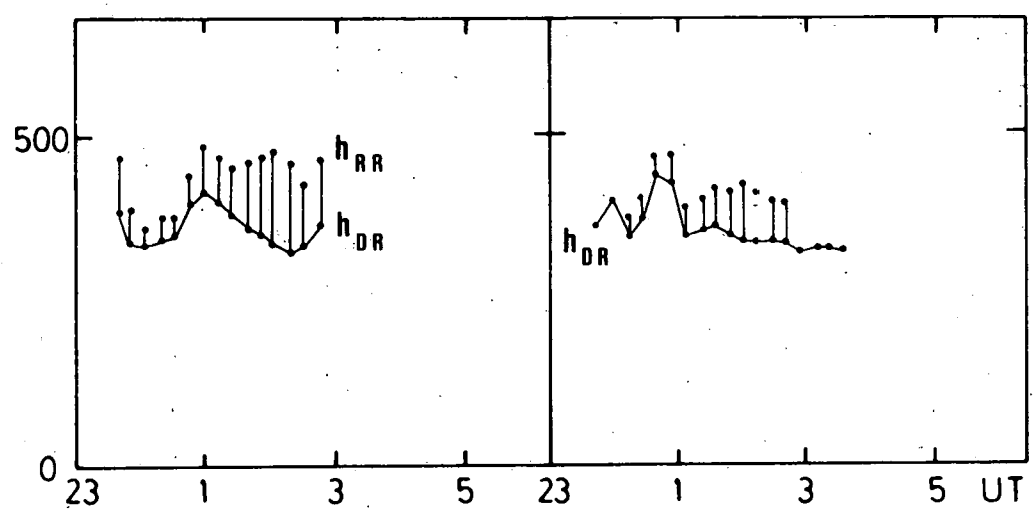

Fig. 7.- For western and estern sections are shown : deduced height of peak dissociative recombination and, on top of vertical bars, deduced height of peak IR emission.

ACKNOWLEDGEMENTS

M. Fafiotte is largely responsible for the high quality of the measurements.

We also thank M.C. Pantalacci for her help at various stages of elaboration of this paper.

The experiment was carried out within the Scientific Program of Centre National d'Etudes Spatiales. We are grateful to this organization for carrying out the campaign.

QUESTION (F.E. ROACH).

Can you say anything about a comparison between your results near the South Atlantic anomaly and similar results away from the anomaly ?

Reply.- Balloon observations of that kind are yet unique. We observe at this stage no effect obviously connected with the induction anomaly or related particle precipitation. The longitude areas observed here (about 35° and 65° West) show different behaviours probably connectted with neutral winds and the different declination. It is yet difficult to generalize as the night was magnetically disturbed.

QUESTION (M.J. SEATON)

What is the process responsible for the permitted oxygen lines ?

Reply.- Peak electron densities were above 10^6 el. cm^{-3}, radiative recombination $O^+ + e^-$ is on adequate source. The optimal correlation of R^2/IR is in favour that process.

$O^+ + O^-$ has also been proposed as a competitive process. It would be more difficult to reconcile with the large spatial separations observed.

REFERENCES

1. a) BARBIER D. et GLAUME J., *C.R. Acad. Sci.*,**250**, 2043, 1960.
   b) BARBIER D. et GLAUME J., *Ann. Geophys.*, **16**, 319, 1960.
   c) BARBIER D., WEILL G. et GLAUME J., *Ann. Geophys.*, **17**, 305, 1961.
2. a) REED E.I., FOWLER W.B. and BLAMONT J.E., *J. Geoph. Res.*, **78**, 5658, 1973.
   b) THUILLIER G., *Thèse* Paris VI, 1973.
3. INGHAM M.F., *Monthly Notices of the Royal Astronomical Society*, **124**, 505, 1962.
4. HICKS G.T. and CHUBB T.A., *J. Geoph. Res.*, **75**, 6233, 1970.
5. WEILL G. et JOSEPH J., *C.R. Acad. Sci.*, **271**, 1013, 1970.
6. TINSLEY B.A., *Ann. Geoph.*, **28**, 155, 1972.
7. HANSON W.B., *J. Geoph. Res.*, **74**, 4343, 1969.
8. KNUDSEN W.C., *J. Geoph. Res.*, **75**, 3862, 1970.
9. TINSLEY B.A. et al., *J. Geoph. Res.*, **78**, 1174, 1973.
10. ACKERMAN M., FAFIOTTE M., LIPPENS C., WEILL F. et VAN RANSBEECK E., *Aeronomica Acta* , C n° **38**, 1974.
11. DESSLER A.J., *J. Geoph. Res.*, **64**, 713, 1959.
12. MARKHAM T.P. and ANCTIL R.E., *J. Geoph. Res.*, **71**, 997, 1966.
13. VAN ZANDT T.E., CLARK W.L. and WARNOCK J.M., *NOAA TR ERL* 222-AL 6, 1972.
14. MARKHAM T.P., BUCHAU J., ANCTIL R.E. and NOXON J.F., *J. Atmos. Terr. Phys.*, **37**, 65, 1975.
15. TINSLEY B.A. and BITTENCOURT J.A., *J. Geoph. Res.*, **80**, 2333, 1975.
16. CHANDRA S., REED E.I., MEIER R.R., OPAL C.B. and HICKS G.T., *J. Geophy. Res.*, **80**, 2327, 1975.